

Continuous Spectroscopic and Redox Tuning of Dinuclear Compounds: Chlorotetrakis(μ -N,N'-diarylformamidinato)diruthenium(II, III)¹

Chun Lin, Tong Ren,* Edward J. Valente,[†] Jeffrey D. Zubkowski,^{††} and Eugene T. Smith
 Department of Chemistry, Florida Institute of Technology, Melbourne, FL 32901, U. S. A.

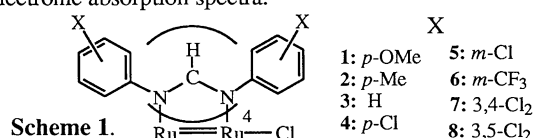
[†]Department of Chemistry, Mississippi College, Clinton, MS 39058, U. S. A.

^{††}Department of Chemistry, Jackson State University, Jackson, MS 39217, U. S. A.

(Received March 28, 1997; CL-970233)

The color of the $\text{Ru}_2(\mu\text{-N,N'}\text{-diarylformamidinato})_4\text{Cl}$ series displays a dramatic red-shift as the electron-withdrawing power of aryl-substituent is increased.

Electronic tuning of dinuclear paddlewheel compounds² is of interest since certain catalytic properties of these compounds, such as the carbene-transfer reaction by dirhodium and the oxygenation reaction by dicopper,³ are complementary to those of mononuclear coordination compounds. It has been established for mononuclear species that remote substituents (those away from the first coordination sphere) can greatly influence redox,⁴ photophysical,⁵ and catalytic properties.⁶ We are interested in the fine tuning of both the electronic structure and the reactivity of dinuclear paddlewheel compounds through remote substituents, and the linear free energy relationship therein. Studies of both the dimolybdenum(II) and dinickel(II) compounds supported by diarylformamidinates revealed that while the reduction potential ($E_{1/2}(\text{M}_2^{5+}/\text{M}_2^{4+})$), and hence the $E(\text{HOMO})$, linearly correlates with the Hammett constant of aryl-substituents in both series, the electronic absorption spectra remain identical within each series, which implies a substituent-independent distribution of upper-valence molecular orbitals.⁷ We describe herein the results from the series of mixed valence diruthenium(II,III) compounds supported by diarylformamidinates (Scheme 1), where significant attenuation has been achieved for both the redox potentials and the electronic absorption spectra.



Novel diruthenium(II,III) compounds **1**, **4** - **8** and the known compounds **2** and **3** were prepared by either treating $\text{Ru}_2(\text{OAc})_4\text{Cl}$ with excess formamidine at elevated temperature, or refluxing $\text{Ru}_2(\text{OAc})_4\text{Cl}$, formamidine, Et_3N , (molar ratio 1:8:4), and excess LiCl in THF. All the compounds have been purified by either recrystallization or flush column chromatography, and analyzed satisfactorily.⁸ A preliminary X-ray diffraction study of **1**·0.5 CH_2Cl_2 ⁸ revealed a paddlewheel arrangement of four bridging formamidinates around the Ru_2 core and an axial chloro ligand (ORTEP not shown). Key metric parameters for **1**, Ru-Ru, Ru-Cl, and averaged Ru-N bond lengths are respectively 2.390, 2.433 and 2.070 Å, which are comparable to those reported for the known compounds **2** and **3**.⁹ The room temperature magnetic moment varies between 3.64 and 3.97 Bohr magneton across the series, which is indicative of an $S = 3/2$ ground state. Therefore, the compounds in the current series are isoelectronic with $\text{Ru}(\text{O}_2\text{CR})_4\text{Cl}$, and the electronic configuration for Ru_2 core is best described as $\sigma^2\pi^4\delta^2(\delta^*\pi^*)^3$.²

One of the striking features of the current series is the color of

the respective CH_2Cl_2 solutions, which gradually change from dark green for **1** - **3** to burgundy red for **7** and **8**. The origin of this red-shift is obvious from the UV-vis spectra: while all the compounds exhibit three bands of very similar λ_{max} (Table 1), i.e. around 272 nm (I), 470 nm (II), and 580 nm (III, **1** - **5** only), the fourth band (IV) appears as a well-resolved peak for **1** at 688 nm and **2** at 680 nm, and slowly becomes a shoulder as it merges with band III (Figure 1). Analogously to the

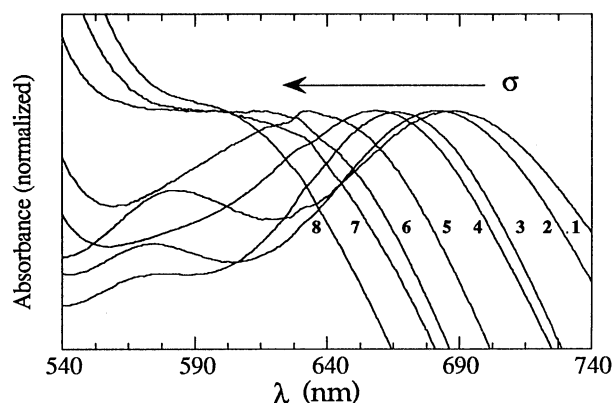


Figure 1. Band IV of the electronic absorption spectra of compounds **1** - **8**.

isoelectronic species $\text{Ru}_2(\text{O}_2\text{CR})_4\text{Cl}$,¹⁰ bands I-IV are tentatively assigned as the $\pi(\text{Cl}) \rightarrow \pi^*(\text{Ru}_2)$ LMCT, $\pi(\text{Ru-N}, \text{Ru}_2) \rightarrow \pi^*(\text{Ru}_2)$, $\pi^*(\text{Ru}_2) \rightarrow \sigma^*(\text{Ru-N})$, and $\delta(\text{Ru}_2) \rightarrow \pi^*(\text{Ru}_2)$ transitions, respectively. The substituent-independence of bands I-III parallels the trend observed for both the dimolybdenum and the dinickel series,⁷ and indicates that substituent perturbations on most of the valence orbitals are essentially the same. The substituent-dependence of band IV may originate from the difference in either the orbital energy or the configuration energy.¹¹ A satisfactory linear relationship exists between the transition energy of band IV (E_{IV} in cm^{-1}) and the Hammett constant (σ): $E_{\text{IV}}(\text{X}) - E_{\text{IV}}(\text{H}) = \rho \cdot \Sigma \sigma = 269(8\sigma)$ (cm^{-1}) with a correlation coefficient of 0.987. To our knowledge, this is the first example of linear spectral tuning for a M-M bonded species.

The rich redox-chemistry in the current series is exemplified by the cyclic voltammograms (CV) of **1** shown in Figure 2. There are three distinctive redox processes in the CV recorded with the non-coordinating electrolyte $\text{Bu}_4\text{N-BF}_4$ (Figure 2a) and their assignments are depicted in Scheme 2. While these assignments are consistent with that for **3**,⁹ the mechanism is somewhat different. The first peaks (I) correspond to the $[\text{Ru}_2(\text{L})_4\text{Cl}]^{+/0}$ couple and are (quasi)reversible throughout the series (see Table 1). The second wave (II) is associated with the

Table 1. Experimental Results for $[\text{Ru}_2(\text{ArNCHNAr})_4\text{Cl}]$

Compound	1	2 ^a	3 ^a	4	5	6	7	8
$E_{1/2}(\text{I})/\text{mV}$, ($i_{\text{pa}}/i_{\text{pc}}$) ^b	518 (0.93)	565 (1.09)	684 (0.99)	854 (1.49)	947 (1.43)	1068 (1.82)	1106 (0.95)	1212 (1.41)
$E_{\text{pc}}(\text{II})/\text{mV}$, ($i_{\text{pa}}/i_{\text{pc}}$) ^b	-751 (NA)	-706 (NA)	-590 (NA)	-410 (NA)	-330 (NA)	-343 (0.31)	-254 (0.34)	-228 (0.58)
$E_{\text{pa}}(\text{III})/\text{mV}$ ^b	-82	43	58	227	309	447	460	660
$\lambda_{\text{max}}/\text{nm}$ ($\epsilon/\text{M}^{-1}\text{cm}^{-1}$) ^c	688 (2580)	680 (3350)	666 (2490)	656 (2160)	633 (2170)	622 (2610)	610 (3120)	601 (3340)
	583 (2360)	580 (2880)	576 (2070)	583 (1930)				
	471 (4035)	467 (5360)	462 (5460)	472 (4570)	475 (4640)	473 (6060)	489 (5690)	494 (6530)
	271 (52700)	274 (50300)	273 (40200)	270 (43300)	272 (43700)	274 (45600)	271 (52100)	271 (46900)

^a Data re-determined in this work; ^b Measured in CH_2Cl_2 with Bu_4NBF_4 as supporting electrolyte, Pt working and auxiliary electrodes, Ag/AgCl reference electrode, $[\text{Ru}_2] \approx 1 \text{ mM}$, and scan rate 100 mV/s ; $E_{1/2}(\text{Fc}^+/\text{Fc})$ was consistently measured at $+625 \text{ mV}$; ^c UV-Vis spectra were recorded in anhydrous CH_2Cl_2 .

$[\text{Ru}_2(\text{L})_4\text{Cl}]^{0/-}$ couple, and appears irreversible for most compounds (the anodic peak was observed only for **6** - **8**). The apparent irreversibility originates from a chemical step following electron transfer, namely the facile dissociation of Cl^- from $[\text{Ru}_2(\text{L})_4\text{Cl}]^-$ generated at the cathode. The $i_{\text{pa}}/i_{\text{pc}}$ ratio for II increases with increasing σ , indicating an increasing affinity of $\text{Ru}_2(\text{II},\text{II})$ core for axial Cl^- across the series. A set of peaks (III) at more positive potential (compared with II) is ascribed to the axial-chloro-free $[\text{Ru}_2(\text{L})_4]^+/\text{Ru}_2(\text{L})_4$ couple. A distinctive anodic peak is observed for all the compounds, confirming a significant production of $\text{Ru}_2(\text{L})_4$ at the expense of $[\text{Ru}_2(\text{L})_4\text{Cl}]^-$. In contrast, the cathodic current for III is very small and only observable for **1** - **3**, revealing a limited tendency of Cl^- dissociation for $\text{Ru}_2(\text{II},\text{III})$. The assignment of the coupled reactions revealed by waves II and III is clearly demonstrated via a Cl^- titration experiment: upon the completion of the CV scan shown in Figure 2a, CVs were recorded for the solution titrated with $1 \text{ M Et}_4\text{NCl}$ (in CH_2Cl_2). The waves associated with III gradually reduced with the addition of Et_4NCl and eventually vanished (Figure 2b, $[\text{Cl}^-]/[\text{Ru}_2] \approx 100$) due to the elimination of

$\text{Ru}_2(\text{L})_4$ from the bulk solution. As an independent proof of the mechanism, the CV shown in Figure 2a was reproduced by numerical simulation.¹²

Linear least-squares fitting of $\Delta E_{1/2}(\text{I})$ and $\Delta E_{\text{pc}}(\text{II})$ vs σ according to the equation $\Delta E = E(\text{X}) - E(\text{H}) = \rho \cdot (8\sigma)$ yield the reactivity constants 88.9 mV (ρ_{I} , correlation coefficient $R = 0.994$) and 69.3 mV (ρ_{II} , $R = 0.985$) for reactions I and II, respectively. These reactivity constants are of the same magnitude as that of dimolybdenum(II) (87 mV) and dinickel(II) (114 mV) analogs.⁷

In summary, while the compounds in the current series possess the same electronic configuration, both the energies of their frontier orbitals and their optical properties depend significantly on the remote substituents. Furthermore, the affinity of both $\text{Ru}_2(\text{II},\text{III})$ and $\text{Ru}_2(\text{II},\text{II})$ cores towards axial Cl^- increases with increasing σ , which may find interesting application in dinuclear catalysts utilizing the axial position(s) as the active site.³

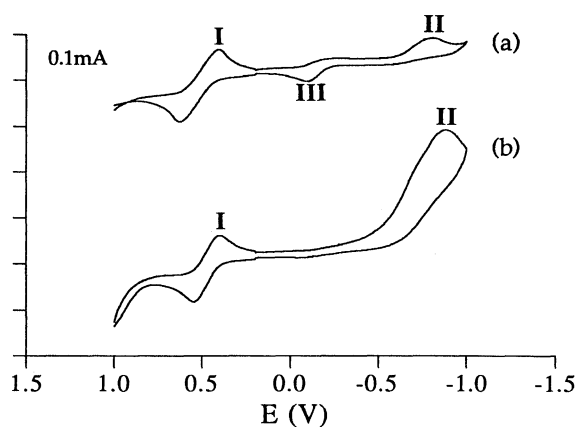
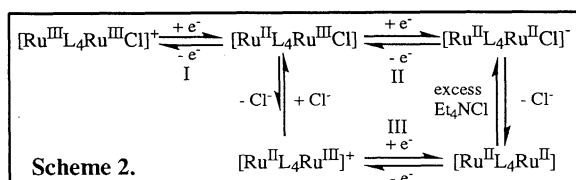


Figure 2. Cyclic voltammograms of **1**. (a) recorded with Bu_4NBF_4 ; (b) recorded with Bu_4NBF_4 and excess Et_4NCl . See text and Table 1 for the experimental conditions.

References and Notes

- Part 4. Linear Free Energy Relationships in Dinuclear Compounds. See reference 7 for Parts 1 - 3.
- F. A. Cotton and R. A. Walton, "Multiple Bonds between Metal Atoms"; Second ed.; Oxford University Press, Oxford (1993).
- For Rh_2 see M. P. Doyle, *Aldrichimica Acta*, **29**, 3 (1996); A. Padwa and D. J. Austin, *Angew. Chem. Int. Ed. Engl.*, **33**, 1797 (1994); For Cu_2 , see S. Minakata, E. Imai, Y. Ohshima, K. Inaki, I. Ryu, M. Komatsu, and Y. Ohshiro, *Chem. Lett.*, **1996**, 19.
- K. M. Kadish, *Prog. Inorg. Chem.*, **34**, 435 (1986).
- S. D. Cummings and R. Eisenberg, *J. Am. Chem. Soc.*, **118**, 1949 (1996).
- For recent examples, see F. C. Rix, M. Brookhart, and P. S. White, *J. Am. Chem. Soc.*, **118**, 2436 (1996); K. Kato, T. Yamada, T. Takai, S. Inoki, and S. Isayama, *Bull. Chem. Soc. Jpn.*, **63**, 179 (1990); E. N. Jacobsen, W. Zhang, and M. L. Guler, *J. Am. Chem. Soc.*, **113**, 6703 (1991); S.-B. Park, K. Murata, H. Matsumoto, and H. Nishiyama, *Tetrahedron: Asymmetry*, **6**, 2487 (1995).
- C. Lin, J. D. Protasiewicz, E. T. Smith, and T. Ren, *J. Chem. Soc., Chem. Commun.*, **1995**, 2257 and *Inorg. Chem.*, **35**, 6422 (1996); C. Lin, J. D. Protasiewicz, and T. Ren, *Inorg. Chem.*, **35**, 7455 (1996).
- Results of elemental analysis and crystallographic study (submitted as supplementary materials) are available from TR.
- F. A. Cotton and T. Ren, *Inorg. Chem.*, **34**, 3190 (1995); J. L. Bear, B. Han, S. Huang, and K. M. Kadish, *Inorg. Chem.*, **35**, 3012 (1996).
- V. M. Miskowski and H. B. Gray, *Inorg. Chem.*, **27**, 2501 (1988).
- A plausible explanation is that as the σ (substituent) increases, the $E(\delta)$ decreases much faster than the $E(\pi^*)$ due to larger ligand contribution to the former orbital.
- Numerical simulation was carried out with DigiSim Version 2.1 (BAS, West Lafayette, IN 47906, USA). The simulated CV is submitted as the Supporting Information.